Space-time resolved quantum field approach to Klein tunneling dynamics across a finite barrier

M. Alkhateeb* and A. Matzkin

Laboratoire de Physique Théorique et Modélisation,

CNRS Unité 8089, CY Cergy Paris Université,

95302 Cergy-Pontoise cedex, France

Abstract

We investigate Klein tunneling with space-time resolved solutions to relativistic quantum field equations. We show in particular that no particle actually tunnels through a finite supercritical barrier, even in the case of resonant tunneling. The transmission is instead mediated by modulations in pair production rates at each edge of the barrier caused by the incoming electron. We further examine the effect of the barrier's width on the numbers of produced pairs in the fermionic case (characterized by saturation) and in the bosonic case (characterized by exponential superradiance).

^{*}Electronic address: mohammed.alkhateeb@cyu.fr

Vacuum pair production in a strong supercritical external field is one of the basic elementary processes predicted by relativistic quantum theory [1]. Understanding its precise dynamics is important not only for fundamental reasons, but also due to current efforts aiming to experimentally observe pair production in the intense laser facilities currently under construction [2, 3]. To this end, several works employing different approaches have examined field configurations that would optimize pair production [4–6].

A related aspect concerns the interaction of a charged particle with the pair production process as the particle scatters on an inhomogenous supercritical field. This is well-known to give rise to "Klein tunneling" [7], that in a first quantized framework appears as undamped propagation inside the potential region. The precise dynamics of this interaction has remained controversial even in the case of a simple electrostatic step, a situation giving rise to the so-called Klein paradox [8]. Time-independent first quantized approaches are generally misleading [9], but even stationary quantum field theory (QFT) methods failed to reach consensus (e.g. the choice of asymptotic "in" and "out" fields [10–13]). A numerical space-time resolved QFT approach [14] was instrumental in computing the precise dynamics of the interaction between the incoming particle and the pair production for a step, leading to a reinterpretation of the fermionic Klein paradox in terms of Pauli blockade of vacuum pair production.

For a particle impinging on a supercritical electrostatic barrier of finite width, the computation of the time-dependent pair creation rates and of the dynamics inside the barrier is expected to be more involved; in particular the asymptotic field operators only contain particles, which has lead some authors [7, 15] to conjecture that a symmetric supercritical barrier once formed cannot radiate. While genuine Klein tunneling has yet to be observed for elementary particles, the physics encapsulated in the first quantized Dirac equation has been used as an effective model in other areas, leading to the experimental observation of Klein tunneling in graphene heterojunctions [16], with trapped ions [17] or cold quantum gases [18].

In this work, we implement a time-dependent space-resolved QFT treatment in order to compute the detailed dynamics of Klein tunneling for fermions and bosons across a finite barrier. In the fermionic case, we will see how vacuum pair production is affected by the exchange symmetry interaction due the positrons' motion inside the barrier, leading indeed to a saturation of the number of produced pairs. We will also show that when an incoming

particle scatters on a barrier, no particle actually tunnels inside, even in the resonant case of nearly full transmission across the barrier; rather, an incoming charge modulates the pair production rate at the left edge of the barrier; this modulation propagates inside the barrier and increases pair production when hitting the right edge. In the bosonic case, a barrier amplifies pair production, with the anti-boson charge oscillating inside the barrier increasing exponentially each time it scatters on an edge.

The barrier is modeled as a one-dimensional background external field with negligible backreaction [19]. The fermionic pair production rate is obtained from field operators Ψ expanded as

$$\Psi(x,t) = \int dp \left(b_p(t)\phi_p(x) + d_p^{\dagger}(t)\varphi_p(x) \right). \tag{1}$$

 ϕ_p and φ_p are resp. the positive and negative energy spinor eigenfunctions of the field-free Dirac Hamiltonian $H_0 = -i\hbar c\alpha_x \partial_x + \beta mc^2$ with eigenvalues $\pm |E_p| = \pm \sqrt{p^2c^2 + m^2c^4}$ (α and β are the usual Dirac matrices [32], m the electron mass and c the light velocity) $b_p(t)$ (resp. $d_p(t)$) is the annihilation operator for a particle (resp. antiparticle), and $b_p^{\dagger}(t)$ and $d_p^{\dagger}(t)$ are the corresponding creation operators obeying the usual commutation relations, i.e. the only non-zero equal time anti-commutators are $[b_p, b_k^{\dagger}]_+ = [d_p, d_k^{\dagger}]_+ = \delta(p-k)$. The time-dependence of the creation and annihilation operators is obtained by noting that Ψ obeys the Dirac equation with the full Hamiltonian $H = H_0 + V(x)$ where V(x) is the background potential. It then follows that [20]

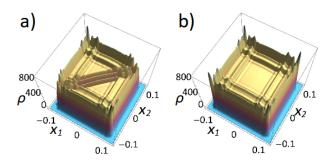


Figure 1: (a) The spatial density $\rho(x_1, x_2)$ of positron couples at positions x_1 and x_2 created inside the barrier at time 2×10^{-3} expressed in atomic units (a.u., defined by $\hbar = m = 1, c = 137.036$, where m is the electron mass); the barrier has width L = 0.2 a.u., height $V_0 = 3mc^2$ and the smoothness has been set to $\epsilon = 0.3/c$. (b) Same as (a) but without the exchange interaction terms in the computations, see Eq. (5).

$$b_p(t) = \int dk \left(U_{\phi_p \phi_k}(t) b_k(0) + U_{\phi_k \varphi_p}(t) d_p^{\dagger}(0) \right)$$
 (2)

$$d_p^{\dagger}(t) = \int dk \left(U_{\varphi_p \phi_k}(t) b_k(0) + U_{\varphi_p \varphi_k}(t) d_p^{\dagger}(0) \right). \tag{3}$$

The time-evolved amplitudes, defined by $U_{\phi_k\varphi_p}(t) \equiv \langle \phi_k | \exp(-iHt/\hbar) | \varphi_p \rangle$ are computed numerically on a discretized space-time grid by relying on a split operator [21] method (the evolution operator is split into a kinetic part propagated in momentum space and a potential-dependent part solved in position space).

Let us first consider vacuum pair production in a quasi rectangular potential barrier of width L; for definiteness we take $V(x) = \frac{V_0}{2} \left[\tanh((x + L/2)/\epsilon) - \tanh((x - L/2)/\epsilon) \right]$ where $V_0 > 2mc^2$ is supercritical and ϵ is a smothness parameter. The electron density is obtained from the vacuum expectation value $\rho_{el}(x,t) = \langle 0|\Psi_{el}^{\dagger}(x,t)\Psi_{el}(x,t)|0\rangle$, where Ψ_{el} is the positive energy part of Eq. (1). The positron density $\rho_{pos}(x_1, x_2, t)$ is obtained similarly from Ψ_{pos} defined as the positive energy part of the field conjugate to the one given by Eq. (1) [22]. Note that physically ρ_{pos} corresponds to the positron density measured in an experiment in which V(x) would be instantaneously switched off.

Since a potential of the form V(x) typically creates two pairs simultaneously (one at edge of the barrier, where the field is highly inhomogeneous), it is particularly instructive to compute the 2-particle density for a joint electron or positron creation at x_1 and x_2 ,

$$\rho_{\rm a}(x_1, x_2, t) = \langle 0 | \Psi_{\rm a}^{\dagger}(x_1, t) \Psi_{\rm a}^{\dagger}(x_2, t) \Psi_{\rm a}(x_2, t) \Psi_{\rm a}(x_1, t) | 0 \rangle / 2!$$
(4)

wherte 'a' stands for pos or el. Note that by construction $\rho(x_1, x_2)$ also counts the number of multiple pairs created on the same edge of the barrier, although the probability for multiple pair creations at a single field inhomogeneity is expected to decrease exponentially as the multiplicity number increases [23, 24] (but see [25]). The two-particle density (4) can be shown to be written as

$$\rho_{\mathbf{a}}(x_1, x_2, t) = \rho_{\mathbf{a}}(x_1, t)\rho_{\mathbf{a}}(x_2, t)/2 - \rho_{\mathbf{a}}^{int}(x_1, x_2, t), \tag{5}$$

indicating that the number of created pairs is affected by the exchange interaction terms encapsulated in ρ^{int} . This is portrayed in Fig. 1 for the positron density inside the barrier. As the positrons produced at each edge propagate towards the opposite side, ρ_{pos}^{int} becomes of

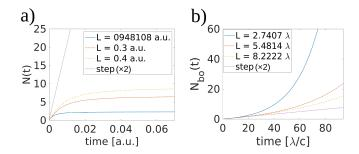


Figure 2: (a) Time-dependence of the total number of created electron-positron pairs N(t) for a fermionic barrier with the parameters given in Fig. 1 except for the width L, indicated in the legend. The rate vanishes except in the limit of a potential step (note that in order to compare the step and finite barrier cases, the curve shown for a step has been multiplied by two). (b) The total number of created boson-anti-boson pairs $N_{bo}(t)$ for a massive bosonic field obeying the Klein-Gordon equation interacting with a background potential barrier with $V_0 = 3m_{bo}c^2$, $\epsilon = 0.3/c$, and varying widths; m_{bo} is the boson mass which renormalizes the atomic units, so that L and t are given in units of $\lambda = m_{bo}\hbar/c$ and λ/c respectively.

the same order of magnitude as the factorized density $\rho_{pos}(x_1)\rho_{pos}(x_2)$, so that the exchange interaction significantly reduces the number of couples inside the barrier.

The number N(t) of created positron-electron pairs, obtained by integrating either $\rho_{pos}(x,t)$ or $\rho_{el}(x,t)$ over all space (i. e. essentially inside the barrier for ρ_{pos} , outside for ρ_{el}) is shown in Fig. 2(a) for different barrier widths. N(t) is seen to saturate after a transient time that depends on the barrier width: at short times the number of produced pairs increases similarly to a step potential, but a fermionic symmetric barrier will not radiate after this transient period, as expected from the asymptotic behavior of the evolution amplitudes $U_{\phi_k\varphi_p}(t)$ [26].

We can now examine how an electron colliding on the supercritical barrier interacts with the fermionic pair production process. We will consider resonant Klein tunneling, that has been widely investigated in the condensed matter analog of quasi-particles undergoing nearly full transmission through electro-static barriers in graphene [27]. The field operators are again given by Eqs. (1)-(3), but the spatial densities are obtained from the expectation values

$$\rho_{\mathbf{a}}(x) = \langle \zeta | \Psi_{\mathbf{a}}^{\dagger}(x) \Psi_{\mathbf{a}}(x) | \zeta \rangle \tag{6}$$

where $|\zeta\rangle = \int dp \zeta_p(p_0, x_0) b_p^{\dagger}(0) |0\rangle$ represents the initial electron wavepacket centered at x_0 with mean momentum p_0 ; for definiteness we take $\zeta_p(p_0, x_0) \propto e^{-\Delta^2(p-p_0)^2 - ipx_0/\hbar}$ corresponding to a Gaussian wavepacket of width Δ , similarly to previous works dealing with the Klein paradox due to a potential step [14, 28]. The resonant barrier condition

$$\left(p_0^2 + V^2/c^2 - 2V\sqrt{p_0^2/c^2 + m^2}\right)^{1/2} = \frac{k\pi}{2L}$$
 (7)

(which holds for a rectangular barrier, corresponding to the potential slope parameter $\epsilon \to 0$) is obtained by maximizing the transmitted Dirac current relative to the incident one (k is an integer). In the first quantized approach, this means that the transmission amplitude $T(p_0)$ for stationary solutions of the Dirac equation is unity, so that if the wavepacket is sufficiently narrow in momentum, it will nearly entirely tunnel through the barrier [9].

However in the present more fundamental second quantized framework, the incoming electron interplays with the particles created by the supercritical potential. The electronic spatial density given by Eq. (6) can be shown to take the form, by using Eqs. (1)-(3), $\rho_{el} = \langle 0 | \Psi_{el}^{\dagger} \Psi_{el} | 0 \rangle + \rho_{el}^{\zeta} \text{ where}$

$$\rho_{el}^{\zeta}(x) = \left| \int dp dk \zeta(p) U_{\phi_k \phi_p}(t) \phi_k(x) \right|^2 \tag{8}$$

gives the evolution of the wavepacket density. Inside the barrier the electron density vanishes (hence there is no electron wavepacket) and the positron density reads

$$\rho_{po}(x,t) = \langle 0| \Psi_{po}^{\dagger}(x,t) \Psi_{po}(x,t) |0\rangle - \rho_{po}^{\zeta}(x,t), \tag{9}$$

where the last term

$$\rho_{po}^{\zeta}(x) = \left| \int dp dk \zeta(p) U_{\varphi_k \phi_p}(t) \varphi_k(x) \right|^2 \tag{10}$$

appears as a correction to the vacuum positron density due to the incoming electron scattering on the supercritical potential.

In the case of resonant Klein tunneling, the barrier needs to be narrow relative to the wavepacket width, so this decrease will be small, but it is nevertheless crucial in order to modulate pair production at the right edge of the barrier. Indeed, most of the wavepacket will typically reach the barrier at times for which the pair production rate becomes negligible. The mechanism invoked in Ref. [14] explaining the positron density depletion for a supercritical step as the result of Pauli blockade should be parsed differently for a finite

barrier since a sizeable part of the wavepacket will typically reach the barrier at times for which the pair production rate vanishes. A possible mechanism could be the following: (i) the incoming electron annihilates a barrier positron; (ii) the hole instability in the positron density propagates inside the barrier; (iii) upon reaching the right edge, the hole stimulates pair production; (iv) the created electrons at the right edge of the barrier account for the recreated transmitted wavepacket. Note that the hole instability undergoes multiple reflections inside the barrier, with successively decreasing amplitudes [9]. Hence the hole hitting the left edge stimulates pair production and the resulting created electronic charge contributes to the small reflected wavepacket.

Numerical results illustrating resonant Klein tunneling are given in Fig. 3. Each panel shows snapshots at different times. By the time the initial electron wavepacket [Fig.3(a)] reaches the barrier, the pair production rate has already decreased [Fig.3(b)]. A small part of the electron wavepacket is reflected, while the transmitted part annihilates barrier positrons thereby modulating the positron density inside the barrier [Fig. 3(c)]. Note there is no electron inside the barrier (the electron density is vanishingly small). The electron wavepacket is then reformed at the right edge of the barrier [Fig. 3(d)] by pair creation due to the positron modulation. Hence there is no tunneling in Klein tunneling, but a change in the pair creation rate at both edges of the barrier caused by the incoming electron.

The present QFT formalism can be applied similarly to spin-0 bosons obeying the Klein-Gordon equation. The field operators in Eqs. (1)-(3) now obey commutation rules, and the basis functions ϕ_p and φ_p are 2-component solutions of the free Klein-Gordon equation expressed in Hamiltonian form [8]. As is well-known, bosons scattering on a supercritical potential step give rise to superradiance [29], whereby the bosonic amplitude reflected from the step is larger than the incoming one (compensated inside the step by the creation of anti-bosonic amplitude). The same phenomenon in the case of a supercritical barrier is expected to lead to an exponential rate of pair creation, as the anti-bosons created at one edge of the barrier undergo multiple scatterings inside the barrier. Our numerical results, shown in Fig. 2(b) for increasing barrier widths confirm this behavior. For a fixed potential, the momentum distribution of the ejected bosons peaks at $(V_0^2 - 4m^2c^4)^{1/2}/2c$, so the creation rate only depends on the time taken by the anti-bosons to travel from one edge to the other. A similar self-amplification takes place in supercritical wells [30] and can be traced back to the divergent behavior of the scattering amplitudes when interacting with a field

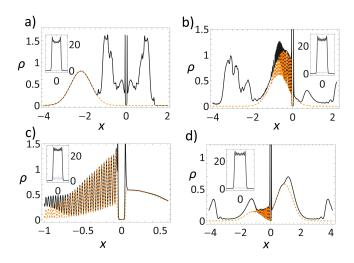


Figure 3: Dynamics of Klein tunneling: an electron wave-packet initially (t=0) centered at x=-3 a.u. to the left of the supercritical barrier is launched with mean momentum $p_0=100$ a.u. The barrier $(V_0=3mc^2,\,\epsilon=0.3/c)$ lies in the region -0.0474 < x < 0.0474 a.u., chosen so that the width L obeys the resonance condition, Eq. (7). (a) Snapshot of particle densities at $t=10^{-2}$ a.u., as the electron wavepacket (dotted-orange line) approaches the barrier. The solid black line gives the total electron density (due to pair creation as well as the wavepacket). The positron density lies outside the scale of the main plot and is shown in the inset (thick grey line); the thin blue line is the contribution of the modulations due to the interaction between the wavepacket and the barrier. (b) Snapshot at $t=3\times 10^{-2}$ a.u. as the wavepacket reaches the barrier. (c) Zoom around the barrier region at $t=4\times 10^{-2}$ a.u., as the electron wavepacket is reformed at the right edge of the barrier; note there is no electron density inside the barrier, but the positron modulations (thin line in the inset) are of greater amplitude. (d) At $t=5\times 10^{-2}$ a.u. most of the wavepacket (dotted orange line) is "transmitted" to the right, while a smaller fraction is reflected

inhomogeneity [31].

Note that in the case of bosonic Klein tunneling, the incoming boson will also undergo aan amplification by multiple scattering inside the barrier; the total anti-boson (ab) density inside the barrier takes the form

$$\rho_{ab}(x,t) = \langle 0| \Psi_{ab}^{\dagger}(x,t) \Psi_{ab}(x,t) |0\rangle + \rho_{ab}^{\zeta}(x,t), \qquad (11)$$

similar to Eq. (9) but with the sign of the modulation inverted relative to the fermionic case. The incoming boson now enhances pair-production when colliding at the left edge of the barrier. The modulation caused by the wavepacket, described by the term ρ_{ab}^{ζ} in Eq.

(11), propagates inside the barrier, amplifying the charge with each collision on a barrier edge on top of the anti-bosonic charge produced by the field.

To sum up, we have investigated Klein tunneling across a supercritical barrier employing a space-time resolved QFT approach. In the fermionic case, the transmitted wavepacket does not tunnel but results from the modulation in pair production produced by the incoming electron. We have also computed the precise dynamics of vacuum pair production by a symmetric background potential, confirming that the number of fermionic pairs saturates while the number of bosons increases exponentially.

- [1] R. Ruffini, G. Vereshchagin and S.-S. Xue, Phys. Rep. 487, 1 (2010)
- [2] G. V. Dunne, Eur. Phys. J. D 55, 327 (2009).
- [3] H. Hu, Contemp. Phys. 61, 12 (2020).
- [4] I. A. Aleksandrov, G. Plunien, and V. M. Shabaev, Phys. Rev. D 94, 065024 (2016).
- [5] J. Unger, S. Dong, Q. Su, and R. Grobe, Phys. Rev. A 100, 012518 –(2019).
- [6] D. D. Su, Y. T. Li, Q. Z. Lv, and J. Zhang, Phys. Rev. D 101, 054501 (2020).
- [7] N. Dombey and A. Calogeracos, Phys. Rep. 315, 41–58 (1999); N. Dombey, P. Kennedy and
 A. Calogeracos, Phys. Rev. Lett. 85, 1787 (2000).
- [8] W. Greiner, B. Müller, and J. Rafelski, *Quantum Electrodynamics of Strong Fields* (Springer-Verlag, Berlin, 1985), Ch. 5 and 10.
- [9] M. Alkhateeb, X. Gutierrez de la Cal, M. Pons, D. Sokolovski and A. Matzkin, Phys. Rev. A 103, 042203 (2021).
- [10] A. I. Nikishov, Phys. At. Nucl. 67 1478 (2004).
- [11] A. Hansen and F. Ravndal, Phys. Scripta 23, 1036 (1981).
- [12] S. P. Gavrilov and D. M. Gitman, Phys. Rev. D 93, 045002 (2016).
- [13] A. Chervyakov and H. Kleinert, Phys. Part. Nuclei 49 374 (2018).
- [14] P. Krekora, Q. Su, and R. Grobe, Phys. Rev. Lett. 92 040406 (2004).
- [15] M. J. Thomson and B. H. J. McKellar, Am. J. Phys. 59, 340 (1991).
- [16] A. Young and P. Kim, Nature Phys 5, 222 (2009).
- [17] R. Gerritsma et al, Phys. Rev. Lett. 106, 060503 (2011).
- [18] T. Salger et al., Phys. Rev. Lett. 107, 240401 (2011).

- [19] S. P. Gavrilov and D. M. Gitman, 101, Phys. Rev. Lett. 130403 (2008).
- [20] T. Cheng, Q. Su, and R. Grobe, Contemp. Phys. 51, 315 (2010).
- [21] M. Ruf, H. Bauke and C. H. Keitel, J. Comp. Phys. 228 9092 (2009).
- [22] S. S. Schweber, An Introduction to Relativistic Quantum Field Theory, (Dover, Mineola, 2005).
- [23] K. Hencken, D. Trautmann, and G. Baur, Phys. Rev. A 51, 998 (1995).
- [24] T. Cheng, Q. Su, and R. Grobe, Phys. Rev. A 80, 013410 (2009).
- [25] Q. Z. Lv and H. Bauke, Phys. Rev. D 96, 056017 (2017).
- [26] M. Alkhateeb and A. Matzkin, in preparation.
- [27] M. I. Katsnelson, K. S. Novoselov and A. K. Geim, Nature Phys. 2, 620 (2006).
- [28] M. Ruf, G. R. Mocken, C. Müller, K. Z. Hatsagortsyan and C. H. Keitel, Phys. Rev. Lett. 102, 080402 (2009).
- [29] C. A. Manogue, Ann. Phys. 181, 261 (1988).
- [30] R. E. Wagner, M. R. Ware, Q. Su, and R. Grobe, Phys. Rev. A 81, 052104 (2010).
- [31] M. Alkhateeb and A. Matzkin, Am. J. Phys. 90, 297 (2022).
- [32] We will consider the usual one effective spatial dimension approximation, neglecting spin-flip and replacing α_x and β by the Pauli matrices σ_1 and σ_3 respectively.